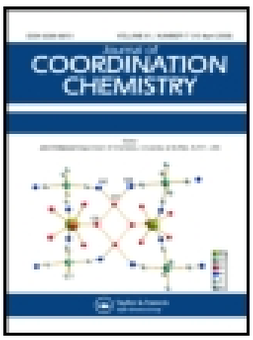

Journal of Coordination Chemistry

ISSN: 0095-8972 (Print) 1029-0389 (Online) Journal homepage: http://www.tandfonline.com/loi/gcoo20

Efficient and versatile catalysis for β-alkylation of secondary alcohols through hydrogen auto transfer process with newly designed ruthenium(II) complexes containing ON donor aldazine ligands

Periyasamy Premkumar, Rajendran Manikandan, Muthukumaran Nirmala, Periasamy Viswanathamurthi & Jan Grzegorz Malecki

To cite this article: Periyasamy Premkumar, Rajendran Manikandan, Muthukumaran Nirmala, Periasamy Viswanathamurthi & Jan Grzegorz Malecki (2017): Efficient and versatile catalysis for β-alkylation of secondary alcohols through hydrogen auto transfer process with newly designed ruthenium(II) complexes containing ON donor aldazine ligands, Journal of Coordination Chemistry, DOI: 10.1080/00958972.2017.1381692

To link to this article: http://dx.doi.org/10.1080/00958972.2017.1381692

Publisher: Taylor & Francis
Journal: *Journal of Coordination Chemistry*
DOI: http://doi.org/10.1080/00958972.2017.1381692

Efficient and versatile catalysis for β-alkylation of secondary alcohols through hydrogen auto transfer process with newly designed ruthenium(II) complexes containing ON donor aldazine ligands

PERIYASAMY PREMKUMAR†, RAJENDRAN MANIKANDAN[#]†, MUTHUKUMARAN NIRMALA†, PERIASAMY VISWANATHAMURTHI*† and JAN GRZEGORZ MALECKI‡

†Department of Chemistry, Periyar University, Salem-636 011, India
‡Department of Crystallography, Silesian University, Szkolna 9, 40-006 Katowice, Poland

A new series of ruthenium(II) carbonyl complexes, $[RuCl(CO)(EPh_3)_2(L_{1\text{-}2})]$ (**1-4**) (E = P or As; H_2L_1 = salicylaldazine, H_2L_2 = 2-hydroxynaphthaldazine), have been assembled from ruthenium(II) precursors $[RuHCl(CO)(EPh_3)_3]$ and bidentate ON donor Schiff base ligands ($H_2L_{1\text{-}2}$). Both ligands and their new ruthenium(II) complexes have been characterized by elemental analyses, spectroscopic methods (UV, IR, NMR (^1H, ^{13}C, ^{31}P) as well as ESI mass spectrometry. The molecular structures of H_2L_1 and **1** have been confirmed by single crystal X-ray diffraction. Based on the above studies, an octahedral coordination geometry around the metal center has been proposed for **1-4**. To investigate the catalytic effectiveness of **1-4**, the complexes have been used as catalysts in *β*-alkylation of secondary alcohols with primary alcohols and synthesis of quinolines. The effect of solvent, time, base, catalyst loading and substituent of the ligand moiety on the reaction was studied. Notably, **1** was a more efficient catalyst towards alkylation of a wide range of alcohols and quinolines synthesis. The reusability of the catalyst was checked and the results showed up to six catalytic runs without significant loss of activity.

Keywords: Aldazine ligands; Ruthenium(II) carbonyl complexes; *β*-Alkylation of alcohols; Synthesis of quinolines

[#]Present address: Department of Chemistry, K. S. Rangasamy college of Arts and Science (Autonomous) Tiruchengode-637215, India
*Corresponding author. Email: viswanathamurthi72@gmail.com

1. Introduction

Alcohols are one of the most important classes of organic compounds owing to their wide variety of uses in industrial and laboratory chemistry. There are many methods for synthesis of alcohols [1]. All of these methods have their own advantages; however, these methods also have disadvantages such as side reactions, tedious work-up procedures, use of toxic reagents and formation of large amounts of inorganic salts as waste. Hence, developing more efficient procedures utilizing nonhazardous and easily available starting materials such as green alkylation methodologies would be desirable for future sustainable processes [2]. The *β*-alkylation of secondary alcohols with primary alcohols is an attractive tool and represents one of the most convenient and straightforward methods for synthesis of coupled secondary alcohols through tandem processes. Recently, less toxic and more readily available alcohols were used as alkylating agents in a greener approach using a metal catalyzed borrowing-hydrogen strategy or hydrogen auto transfer process [3]. This approach is atom economic, thermodynamically favored, proceeds with only water as by-product and follows a cascade redox type pathway involving *in-situ* dehydrogenation of the alcohol to the ketone or aldehyde, followed by aldol reaction resulting in the loss of a water molecule and subsequent hydrogenation of the resulting enone to yield the coupled secondary alcohol as product [4]. Both heterogeneous and homogeneous catalysts promote the *β*-alkylation of secondary alcohols with primary alcohols. In heterogeneous catalysis, cross-coupling reactions of secondary benzylic alcohols with primary alcohols mediated by Pd/C [5], Ag/Al_2O_3 [6] and Au-Pd (hydrotalcite supported) [7] have been investigated. However, the reactions produced coupled ketones as unwanted major products. Various transition metal complexes such as Ir, Rh, Ru, Pd, Cu, Ni and Fe constitute a majority of the homogeneous catalysts because of their high catalytic performance with high product selectivity [8]. Among them ruthenium catalytic systems bearing phosphine ligands have been reported to complete the *β*-alkylation of secondary alcohols with primary alcohols with good yields and selectivity [9]. Heterocyclic compounds like quinoline and its derivatives are extremely versatile compounds, used as building blocks in large number of natural product functional materials, agrochemicals and pharmacological applications [10]. The synthesis of quinoline and its derivatives involved transition metal catalyzed transformations [11]. Particularly ruthenium triphenylphosphine catalyst was used for the synthesis of quinolines in

oxidative coupling of 2-aminobenzyl alcohol with secondary alcohol [11c].

Ligand design is a significant part of synthetic activity because of the subtle control that ligands exert on metal centers to which they are coordinated. Particularly, the choice of ligands is important in stabilization of highly reactive species, unusual oxidation states and implementing catalytic properties. Aldazines are very promising ligands in formation of different coordination compounds because there is wide range of possible substituents. Mostly, they are capable of forming alternate binding sites towards formation of metal complexes [12]. Especially, aldazines containing –C=N–N=C– linkages are versatile building blocks in organic synthesis [13].

In continuation of our research on the synthesis, characterization and catalytic applications of Schiff base transition metal complexes [14, 15], we herein describe synthesis, characterization and catalytic applications of ruthenium(II) complexes bearing Schiff base ligands with ancillary ligands such as triphenylphosphine/triphenylarsine and carbon monoxide. Considering the economic attractiveness and excellent functional group tolerance of ruthenium in homogenous catalysis, we screened the catalytic activity of synthesized complexes in alkylation of alcohols and synthesis of quinolines.

2. Experimental

2.1. *Materials*

All the chemicals were received as analar or chemically pure grade. Solvents were freshly purified and dried according to their standard procedures. $RuCl_3 \cdot 3H_2O$, triphenylphosphine/triphenylarsine and salicylaldehyde/2-hydroxynaphthaldehyde were purchased from Aldrich and used as received. The ruthenium precursors $[RuHCl(CO)(PPh_3)_3]$ and $[RuHCl(CO)(AsPh_3)_3]$ [16] were prepared according to literature methods.

2.2. *General methods*

Microanalyses of carbon, hydrogen and nitrogen were carried out using a Vario EL III elemental analyzer. Infrared spectra of the ligands and the metal complexes were recorded as KBr disks from 4000-400 cm^{-1} using a Nicolet Avatar model FT-IR spectrophotometer. UV-Vis spectra were obtained using a Shimadzu UV-1650 PC spectrometer from 800-200 nm. ^{1}H, ^{13}C and ^{31}P NMR spectra of ligands and complexes were performed in DMSO-*d6* or $CDCl_3$ at room temperature with a Bruker AV400 instrument with chemical shifts relative to tetramethylsilane

or *o*-phosphoric acid as reference. Electrospray ionization mass spectra were recorded by liquid chromatography mass spectrometry quadrupole time-of-flight Micro Analyzer (Shimadzu) at SAIF, Panjab University and Chandigarh. Melting points were checked on a Technico micro heating table and are uncorrected.

2.3. *Synthesis of aldazines (H_2L_{1-2})*

The ligands were prepared by literature method [17]. Typically hydrazine monohydrate (0.048 mL, 1 mmol) was dissolved in methanol (10 mL) and treated with two equivalents of corresponding aldehydes (2 mmol) in methanol (10 mL). The reaction mixture was subsequently refluxed for 2 h and then cooled to room temperature. A yellow crystalline precipitate was formed, which was filtered, washed with methanol (20 mL) and air dried.

2.3.1. Salicylaldazine (H_2L_1). **H_2L_1** was prepared from hydrazine monohydrate (0.048 mL, 1 mmol) and salicylaldehyde (0.212 mL, 2 mmol). Yield: 92% (0.270 g); M.P: 213 °C; Anal. Calc. for $C_{14}H_{12}N_2O_2$: C, 69.99; H, 5.03; N, 11.66%. Found: C, 69.75; H, 5.34; N, 11.78%. IR (KBr, cm^{-1}): 3451 (OH), 1620 (C=N). ^1H NMR (300.13 MHz; $CDCl_3$, ppm): 11.37 (s, 1H, OH), 8.50 (s, 1H, C=N), 6.93-7.39 (m, 8H, ArH). (ESI, *m/z*): 241.2 $[M+H]^+$. Single crystals suitable for X-ray determination were grown by slow evaporation of dichloromethane and chloroform (1:1, v/v) solution of **H_2L_1** at room temperature.

2.3.2. 2-Hydroxynaphthaldazine (H_2L_2). H_2L_2 was synthesized from hydrazine monohydrate (0.048 mL, 1 mmol) and 2-hydroxynaphthaldehyde (0.344 g, 2 mmol). Yield: 89% (0.350 g); M.P: 208 °C; Anal. Calc. for $C_{22}H_{16}N_2O_2$: C, 77.63; H, 4.74; N, 8.23%. Found: C, 77.69; H, 4.54; N, 8.26%. IR (KBr, cm^{-1}): 3462 (OH), 1630 (C=N). ^1H NMR (300.13 MHz; $CDCl_3$, ppm): 13.01 (s, 1H, OH), 8.62 (s, 1H, C=N), 7.38-8.17 (m, 10H, ArH). (ESI, *m/z*): 341.12 $[M+H]^+$.

2.4. *Synthesis of ruthenium(II) complexes (1-4)*

All the new metal complexes were prepared according to the following general procedure. $[RuHCl(CO)(EPh_3)_3]$ (E = P or As) (1 mmol) in methanol (10 mL) was slowly added to chloroform (10 mL) solution of aldazine ligands (**H_2L_{1-2}**) (1 mmol) and heated under reflux for 5-8 h, whereby the solution turned from pale yellow to orange. After reducing the content to half volume and standing for a day, the complexes were obtained as orange precipitates, were filtered and washed several times with ether and dried in *vacuo*.

2.4.1. Synthesis of [RuCl(CO)(PPh_3)$_2$$L_1$]$CH_3CN$ (1). The complex was synthesized from [RuHCl(CO)(PPh_3)$_3$] (0.952 g, 1 mmol) and **H_2L_1** (0.240 g, 1 mmol). Yield: 94% (1.120 g); M.P: 88 °C; Anal. Calc. for $C_{53}H_{43}N_3O_3ClP_2Ru$: C, 65.73; H, 4.48; N, 4.34%. Found: C, 65.75; H, 4.36; N, 4.28%. IR (KBr, cm^{-1}): 3420 (OH), 1964 (C≡O), 1617 (C=N), 1569 (C=N). ^{1}H NMR (300.13 MHz; $CDCl_3$, ppm): 10.5 (s, 1H, OH), 9.4 (s, 1H, C=N), 8.9 (s, 1H, C=N), 7.84-7.78 (m, 15H, ArH), 7.34-7.27 (m, 15H, ArH), 6.93-6.89 (d, 1H, ArH), 6.85-6.82 (t, 2H, ArH), 6.78-6.72 (d, 1H, ArH), 6.68-6.54 (d, 1H, ArH), 6.48-6.42 (d, 1H, ArH), 6.23-6.15 (t, 2H, ArH). ^{13}C NMR (75.47 MHz; $CDCl_3$, ppm): 205.5 (C≡O), 166.2 (C=N), 159.9 (C=N), 153.7 (C–O), 117.2-138.2 (ArC). ^{31}P NMR (162 MHz; $CDCl_3$, ppm): 47.12-49.03. (ESI, *m/z*): 893.4 [M-Cl, CH_3CN]$^+$. Single crystals suitable for X-ray determination were grown by slow evaporation of acetonitrile and chloroform (1:1, v/v) solution of **1** at room temperature.

2.4.2. Synthesis of [RuCl(CO)(PPh_3)$_2$$L_2$] (2). The complex was synthesized from [RuHCl(CO)(PPh_3)$_3$] (0.952 g, 1 mmol) and **H_2L_2** (0.340 g, 1 mmol). Yield: 92% (1.188 g); M.P: 94 °C; Anal. Calc. for $C_{59}H_{46}N_2O_3ClP_2Ru$: C, 71.83; H, 4.50; N, 2.72%. Found: C, 71.57; H, 4.76; N, 2.53%. IR (KBr, cm^{-1}): 3428 (OH), 1936 (C≡O), 1617 (C=N), 1564 (C=N). ^{1}H NMR (300.13 MHz; $CDCl_3$, ppm): 13.1 (s, 1H, OH), 9.7 (s, 1H, C=N), 8.3 (s, 1H, C=N), 7.92-7.73 (m, 15H, ArH), 7.77-7.61 (m, 15H, ArH), 7.58-7.53 (d, 2H, ArH), 7.23-7.15 (d, 2H, ArH), 7.18-7.13 (d, 2H, ArH), 7.08-7.02 (t, 2H, ArH), 6.99-6.95 (t, 2H, ArH), 6.88-6.86 (d, 2H, ArH). ^{13}C NMR (75.47 MHz; $CDCl_3$, ppm): 204.9 (C≡O), 164.6 (C=N), 159.5 (C=N), 154.3 (C–O), 118.1-139.2 (ArC). ^{31}P NMR (162 MHz; $CDCl_3$, ppm): 47.63-49.32. (ESI, *m/z*): 993.19 [M-Cl]$^+$.

2.4.3. Synthesis of [RuCl(CO)($AsPh_3$)$_2$$L_1$] (3). The complex was synthesized from [RuHCl(CO)($AsPh_3$)$_3$] (1.084 g, 1 mmol) and **H_2L_1** (0.240 g, 1 mmol). Yield: 87% (1.151 g); M.P: 98 °C; Anal. Calc. for $C_{51}H_{42}N_2O_3ClAs_2Ru$: C, 62.22; H, 4.16; N, 2.75%. Found: C, 62.48; H, 4.37; N, 2.93%. IR (KBr, cm^{-1}): 3436 (OH), 1942 C≡O, 1625 (C=N) 1570 (C=N). ^{1}H NMR (300.13 MHz; $CDCl_3$, ppm): 11.3 (s, 1H, OH), 10.4 (s, 1H, C=N), 8.7 (s, 1H, C=N), 7.59-7.49 (d, 1H, ArH), 7.64-7.75 (d, 1H, ArH), 7.49-7.35 (m, 15H, ArH), 7.35-7.16 (m, 15H, ArH) 7.16-7.11 (d, 1H, ArH), 7.09-7.05 (d, 1H, ArH) 6.99-6.97 (d, 2H, ArH), 6.95-6.91 (d, 2H, ArH). ^{13}C NMR (75.47 MHz; $CDCl_3$, ppm): 203.8 (C≡O), 165.1 (C=N), 161.6 (C=N), 155.9 (C–O), 192.24-138.24 (ArC). (ESI, *m/z*): 980.16 [M-Cl]$^+$.

2.4.4. Synthesis of [RuCl(CO)($AsPh_3$)$_2$$L_2$] (4). The complex was synthesized from [RuHCl(CO)($AsPh_3$)$_3$] (1.084 g, 1 mmol) and **H_2L_2** (0.291 g, 1 mmol). Yield: 84% (1.155 g); M.P: 110-112 °C; Anal. Calc. for $C_{59}H_{46}N_2O_3ClAs_2Ru$: C, 65.42; H, 4.15; N, 2.81%. Found: C, 65.72; H, 4.32; N, 2.84%. IR (KBr, cm^{-1}): 3427 (OH), 1956 C≡O, 1620 (C=N), 1565 (C=N). ^{1}H NMR (300.13 MHz; $CDCl_3$, ppm): 12.8 (s, 1H, OH), 10.1 (s, 1H, C=N), 9.0 (s, 1H, C=N), 8.70-7.88 (m, 30H, ArH), 7.75-7.64 (m, 4H, ArH), 7.52-7.38 (m, 4H, ArH), 7.37-7.28 (m, 2H, ArH), 7.22-7.17 (t, 1H, ArH), 7.15-7.13 (d, 1H, ArH). ^{13}C NMR (75.47 MHz; $CDCl_3$, ppm): 203.4 (C≡O), 163.9 (C=N), 158.9 (C=N), 156.6 (C–O), 120.1-139.2 (ArC). (ESI, *m/z*): 1080.29 $[M\text{-}Cl]^+$.

2.5. *Crystal structure determination*

Crystals of **H_2L_1** and **1** were mounted on glass fibers for data collection. Crystal data were collected at 295 K using a Gemini A Ultra Oxford Diffraction automatic diffractometer. Graphite monochromated Mo-Kα radiation (λ = 0.71073 Å) was used throughout. The absorption corrections were performed by the multi-scan method. Corrections were made for Lorentz and polarization effects. The structures were solved by direct methods using SHELXS [18]. Refinement and all further calculations were carried out using SHELXL [18]. Hydrogens were included in calculated positions and treated as riding using the SHELXL default parameters. The non-hydrogen atoms were refined anisotropically using weighted full-matrix least squares on F^2. Atomic scattering factors were incorporated into the computer programs.

2.6. *Catalysis*

2.6.1. General procedure for *β*-alkylation of secondary alcohols with primary alcohols. A two-necked 25 mL flask fitted with a reflux condenser and septum was charged with secondary alcohol (2.5 mmol), primary alcohol (2.5 mmol), 1 mol% of ruthenium(II) catalyst, and base KOH (2.5 mmol) in 1,4-dioxane (1 mL). The reaction mixture was heated at 100 °C for 8 h. After completion of the reaction, the mixture was cooled to room temperature, diluted with dichloromethane and hexane mixture and filtered. The filtrate was concentrated *in vacuo* and the resulting residue was purified by column chromatography (hexane/ethyl acetate, 6:4, v/v) to provide the desired product. The products were characterized by ^{1}H and ^{13}C NMR spectroscopy.

2.6.2. General procedure for quinoline synthesis. Catalytic conversion of alcohol to quinoline was carried out using ruthenium(II) complexes as catalysts with the following procedure. The reaction vessel was charged with 2-aminobenzyl alcohol (2.5 mmol), secondary alcohol (2.5 mmol), 1 mol% of ruthenium(II) catalyst and KOH (2.5 mmol) in 1,4-dioxane (1 mL) and the mixture was refluxed at 100 °C for 8 h. After completion of the reaction, the mixture was cooled, diluted with dichloromethane and hexane mixture and filtered. The filtrate was concentrated *in vacuo*, and the resulting residue was purified by column chromatography (hexane/ethyl acetate, 1:1, v/v) to provide the desired product. The products were characterized by ^{1}H and ^{13}C NMR spectroscopy.

3. Results and discussion

3.1. *Synthesis of ligands and metal complexes*

Aldazine ligands (**H_2L_{1-2}**) were synthesized by one step reaction of hydrazine mono hydrate with corresponding aldehydes (scheme 1). The ruthenium complexes $[RuCl(CO)(EPh_3)_2(L_{1-2})]$ (**1-4**) were synthesized by reacting **H_2L_{1-2}** with $[RuHCl(CO)(EPh_3)_3]$ (E = P or As) in equimolar ratio (scheme 2). The isolated complexes are stable in air and soluble in common solvents such as dichloromethane, chloroform, benzene, acetonitrile, ethanol, methanol, DMF and DMSO. All the complexes were characterized by elemental analyses, IR, electronic, NMR, ESI-mass spectral methods and single crystal XRD. Complexes **1-4** generally showed the molecular ion peak with loss of a chloride $[M\text{-}Cl]^+$ (figures S3-S6).

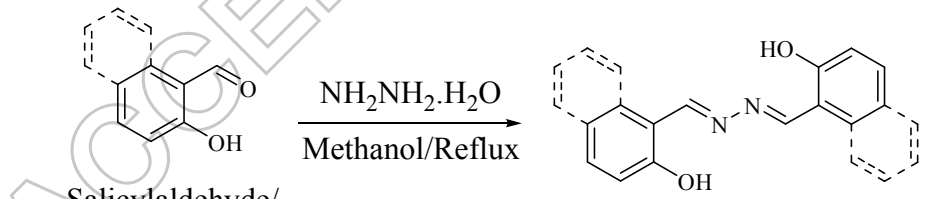

Salicylaldehyde/
2-hydroxynaphthaldehyde

H_2L_{1-2}

Scheme 1. Synthesis of **H_2L_{1-2}**.

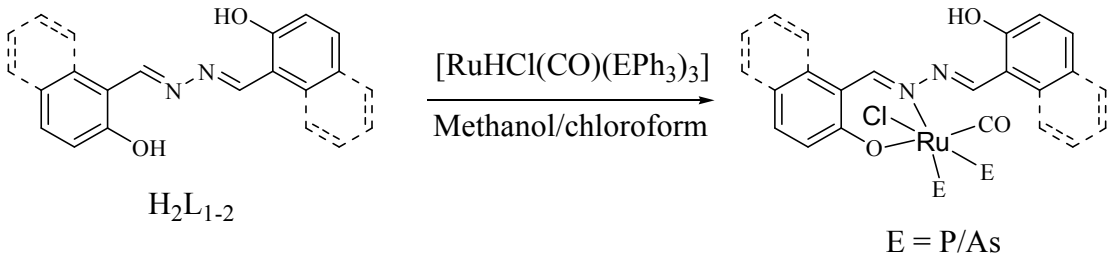

Scheme 2. Synthesis of ruthenium(II) complexes (**1**-**4**).

3.2. *Structural evaluations with spectroscopic studies*

3.2.1. IR spectroscopic analysis. The IR spectra provided significant information about the metal ligand bonding. The peaks at 1630-1624 cm^{-1} in the ligands were assigned to azomethine groups. In complexes, the peak due to $\nu_{C=N(1)}$ shifted to lower frequencies indicating the participation of $\nu_{C=N(1)}$ group in bonding with ruthenium. However, no shift in the frequency of $\nu_{C=N(2)}$ indicates non-participation of C=N(2) in bonding with ruthenium. A strong band at 1320–1300 cm^{-1} in free ligands was assigned to phenolic C–O stretch. One C–O stretch shifted to higher frequency (1390–1360 cm^{-1}) in the complexes, showing coordination through the phenolic oxygen. The complexes display a medium to strong band at 1964-1936 cm^{-1} from coordinated carbon monoxide at slightly higher frequency than in the precursor complexes. Vibrations from PPh_3/$AsPh_3$ were at 1435-1457 cm^{-1}. IR spectra of the complexes confirm the coordination mode of the aldazine ligands to ruthenium(II) *via* one azomethine nitrogen and phenyl oxygen along with the presence of triphenylarsine and triphenylphosphine groups.

3.2.2. Electronic spectroscopic analysis. Electronic absorption spectra of the ligand and complexes (figures S7-S10) have been recorded in dichloromethane solution. The complexes showed intense absorptions from 220-570 nm. The absorption at 400-570 nm is probably due to metal-to-ligand charge transfer. The high energy bands below 370 nm were assigned to ligand-centered transitions. The pattern of the electronic spectra of new ruthenium(II) complexes suggests presence of an octahedral environment around metal center [19].

3.2.3. ^{1}H NMR spectroscopic analysis. ^{1}H NMR spectra of the ligands and complexes (figures S11-S14) show signals in the expected regions. Peaks at 8.6-8.5 ppm in the free ligands are assigned to azomethine protons. In spectra of complexes, two singlets were assigned to

coordinated (10.4-9.4 ppm) and free (9.0-8.3 ppm) azomethine protons. Spectra of free ligands have a peak at 13.1-10.5 ppm, characteristic of phenolic OH. Spectra of free ligands and **1-4** showed a series of overlapping multiplets for aromatic protons at 8.70-6.15 ppm.

3.2.4. ^{13}C NMR spectroscopic analysis. The ^{13}C NMR spectra exhibit the expected signals (figures S15-S17). The complexes exhibit a peak at 205.50-203.4 ppm which is due to terminal C≡O carbon [20]. Two azomethine carbons with a difference in chemical shift values of 5 ppm are observed in all the complexes. The azomethine carbon with higher chemical shift values (166.2-163.9 ppm) can be attributed to azomethine having nitrogen bound to ruthenium. The other chemical shift (161.6-158.9 ppm) can be ascribed to unbound azomethine. The peak at 156.7–152.7 ppm can be attributed to coordinated carbonyl carbon. Peaks for aromatic carbons were at 117.2-139.2 ppm.

3.2.5. ^{31}P NMR spectroscopic analysis. ^{31}P NMR spectra were recorded to confirm the presence of triphenylphosphine groups and their configuration in the complexes. The observation of two sharp singlets around 49.32-47.12 ppm for **1** and **2** indicated that the two triphenylphosphine ligands were *cis* in these complexes (figures S18 and S19).

3.2.6. Single crystal X-ray diffraction studies. Single crystal X-ray diffraction studies of $\mathbf{H_2L_1}$ and **1** confirm the structures suggested from the spectroscopic studies. Details of the data collection, solution and refinement are gathered in the Experimental section and data are presented in tables 1 and 2. The ORTEP view of $\mathbf{H_2L_1}$ (50% probability ellipsoids) along with partial atom numbering scheme is shown in figure 1 and important bond lengths and angles are summarized in table 2.

The perspective view of **1** with atom numbering scheme is depicted in figure 2, while selected bond lengths and angles are given in table 2. Complex **1** crystallized in the monoclinic *P21/c* space group. The coordination geometry around ruthenium is six coordinate with distorted octahedral geometry from coordination of N(1) and O(2) from aldazine ligand, P(1) and P(2) from triphenylphosphine ligands, C(1) from carbonyl ligand and a chloride Cl(1). The ruthenium(II) has a core $RuCl(CO)ONP_2$ coordination environment along with one lattice CH_3CN molecule. In **1**, the *cis* angles are [P(2)−Ru(1)−P(1)] 99.47(2)°, [O(2)−Ru(1)−Cl(1)]

83.20(5)° and [O(2)−Ru(1)−N(1)] 86.78(7)°. The carbonyl group is *trans* to coordinated O(2) [C(1)−Ru(1)−O(2)] with an angle of 177.86(9)°. The PPh_3 ligands are mutually *cis* for better π-interaction; the presence of O(2)−N(1), a stronger π-acidic ligand may have forced the bulky PPh_3 ligands to take *cis* position for steric reasons. The *cis* angles deviate from linearity and O(2)−N(1) (six-membered ring) leads to small [O(2)−Ru(1)−N(1)] bite angle 86.78(7)°. The ruthenium-ligand bond distances, C(1)–Ru(1) 1.839(3), N(1)–Ru(1) 2.110(2), O(2)–Ru(1) 2.0759(17), P(1)–Ru(1) 2.3808(7), P(2)–Ru(1) 2.3594(7), Cl(1)–Ru(1) 2.4459(7), in **1** agree well with that reported for other ruthenium(II) complexes containing triphenylphosphine and the carbonyl group (CO) [21].

3.3. *Catalytic studies*

3.3.1. Catalytic *β*-alkylation of secondary alcohols with primary alcohols. Numerous reports have demonstrated that ruthenium(II) complexes are active catalysts for synthesis of organic compounds. It has also been established that the introduction of Schiff base ligand to the metal center enhances the catalytic activity. To investigate a promising catalytic system, a screen was performed for a model reaction between 1-phenyl ethanol and benzyl alcohol [22]. In order to ascertain optimal reaction conditions, the influence of solvent, base, time and the effect of catalyst concentration on the yield were investigated (table 3). We are interested in exploring the solvent-dependent differences in the activities of catalysts on carrying out the model reaction using toluene, benzene, 1,4-dioxane, acetonitrile, EtOH, H_2O, DMF and DMSO (table 3). Aromatic hydrocarbon solvents such as toluene and benzene (table 3, entries 2 and 3) were better reaction media than polar aprotic (CH_3CN, DMF, DMSO; table 1, entries 5-7) or protic solvents (table 3, entries 8 and 9). Reaction carried out in 1,4-dioxane offered rapid reaction and excellent yield (up to 92%) [23] (table 3, entry 4). Reaction in the absence of base, lowered the reaction yield for *β*-alkylation of alcohols (table 3, entry 10). Weak bases such as Na_2CO_3 and K_2CO_3 were ineffective (table 3, entries 11 and 12). The reaction was accelerated by the addition of strong bases such as KO*t*Bu, $NaNH_2$ and NaOH (table 3, entries 13-15). When the reaction was continually checked using KOH, the yield was excellent (table 3, entry 4 up to 92%). So we choose KOH as the best choice of base for all the reactions. The control experiment was performed for extended time and no further gain in conversion was obtained up to 24 h (table 3, entries 16-18). The role of catalyst was checked without catalyst in the presence of solvent and base. However, the yield of the product is very low (table 3, entry 19).

3.3.1.1. Effect of catalytic efficiency with co-ligands and catalyst loading. We also studied the influence of the substituents and catalyst loading on the catalytic activity. The results are summarized in table 4. Lower catalyst loadings lead to moderate yields and longer reaction times are required to achieve maximum conversion. When the amount of catalyst was increased (table 4, entries 1-3) the product yield increased. Likewise, lowering the catalyst loading had a detrimental impact on reactivity. The ability to use small amounts of catalyst and still achieve high conversions is of importance in alkylation reactions (table 4, entry 3). When the catalyst loading was increased further, there is no improvement in yields (table 4, entry 4). However, it is important to note that complexes with salicylaldehyde substituents and those containing PPh_3 and $AsPh_3$ co-ligands showed the best selectivity toward the synthesis of alcohol (table 4, entries 3 and 5). Thus, electronic properties may also account for the catalytic activity. On the basis of the above optimized conditions, we extended the catalytic alkylations for a variety of secondary alcohols with primary alcohols (table 5) and the formation of alkylated products was confirmed by ^{1}H NMR and ^{13}C NMR spectroscopy (figures S20-S28 and S29-S34).

3.3.1.2. Recyclability of catalyst. For any catalyst system, it is important to observe its ease of partition, recoverability and reusability. The reusability of **1** was investigated using 1-phenyl ethanol and benzyl alcohol as model substrates. After each run, the catalyst was recovered by the addition of dichloromethane and hexane mixture. The catalyst was then thoroughly washed with hexane and dried in air before using in the next run. As shown in figure 3, the catalyst can be efficiently recycled and reused more than six times without significant loss of catalytic activity or selectivity and after that the activity slightly decreases. This may be due to incomplete catalyst recovery in the reaction mixture. When comparing the efficiency of our new catalyst with previously reported literature [2b, 22a, 24], the present catalyst exhibits the finest activity in terms of minimum catalyst loading, mild conditions and short reaction time. In addition the complexes are easier to prepare and cheaper than others.

3.3.1.3. Mechanistic study. The reaction mechanism remains to be elucidated. Nevertheless, some comments can be made from our results and also in accord with literature [25]. Initially, the phosphine ligand is lost to make room for alkoxide attack; subsequent *β*-elimination yields

the anionic metal hydride complex. Although not observed, we propose this species to be the key intermediate of the catalytic process. Anionic hydrides exhibit hydridic reactivity and have been employed in ketone, aldehyde, alkyl halide and acyl chloride reduction. The initially formed *α,β*-unsaturated ketone is first reduced. The reduction might proceed by an associative mechanism in which the aldazine ligand undergoes ring-slippage, to allow substrate coordination to the metal center and subsequent hydride transfer or the reduction might proceed *via* an intermolecular hydride transfer process. In both processes, the *α.β*-unsaturated ketone is activated toward hydride transfer by potassium ion. The hydride is added to the *β*-carbon of the substrate to give the intermediate structure. Then, successive transfer hydrogenation of C=O bond gives the corresponding product.

3.3.2. Quinoline synthesis. Encouraged by the above results, the previously optimized reaction conditions were further applied to the synthesis of quinolines using various alcohols. As can be seen from table 6, all the reactions proceed smoothly and give the corresponding quinolines in good to high yield upon isolation (table 6, entries 1-9). The reaction of 1-phenylethanol and tolylethanol with 2-amino benzylalcohol progressed smoothly to give the corresponding quinoline products in excellent yields under optimized reaction conditions (table 6, entries 1 and 2). Moderate yields of products could be obtained for the reactions involving long chain secondary alcohols (table 6, entries 8 (75%) and 9 (64%)). Unexpectedly, 2-furanylethanol reacted to give the corresponding quinoline in a good yield (table 6, entry 6 (79%)). The reaction of 2-aminobenzyl alcohol with 2-naphthanylethanol formed 2-(naphthalen-2-yl) quinoline in 89% yield (table 6, entry 5). All the products were confirmed by ^{1}H NMR and ^{13}C NMR spectroscopy (figures S35-S37 and S38-S40).

4. Conclusion

Synthesis and characterization of ruthenium(II) carbonyl complexes bearing aldazine functionalized Schiff base ligands are reported. The structures of these complexes were determined by analytical and spectroscopic methods and X-ray single crystal analysis (for $\mathbf{H_2L_1}$ and **1**). Based on analytical and spectral results an octahedral structure was confirmed for the complexes. The catalytic study of **1**-**4** for *β*-alkylation of alcohols was studied and solvent, time, base and catalyst loading were optimized. The results also showed that steric and electronic

effects of the ligands play a role in the catalytic activity of the new complexes. In the *β*-alkylation **1** is a versatile and efficient catalyst under moderate conditions in comparison to its analogues and other transition metal complexes [26]. Also, **1** has high tolerance to functional groups in the quinoline syntheses. These results demonstrate high versatility and potential of aldazine functionalized Schiff base ligands with triphenylphosphine/triphenylarsine co-ligands in homogeneous catalytic reactions. The two catalytic systems were resilient to the use of various substrates and generate minimal waste.

Supporting information

CCDC 1469977 and 1524091 contain the supplementary crystallographic data for this paper. These data can be obtained free of charge *via* http://www.ccdc.cam.ac.uk/conts/retrieving.html, or from the Cambridge Crystallographic Data Centre, 12 Union Road, Cambridge CB2 1EZ, UK; [Fax: +44–1223/150 336033; E-mail: deposit@ccdc.cam.ac.uk]. Representative ESI-MS, UV and NMR (^{1}H, ^{13}C, ^{31}P) spectra of coordination compounds, catalysis protocols, characterization data for *β*-alkylation of alcohols and quinoline synthesized products and selected ^{1}H and ^{13}C NMR spectra of coupling products.

Acknowledgement

One of the authors (P.P.) expresses his sincere thanks to Periyar University, Salem, India for financial support through University Research fellowship. The authors also thank UGC, India for financial assistance to Department of Chemistry, Periyar University, Salem under SAP (No. 540/20/DRS-I/2016(SAP-I)).

References

[1] (a) Q. Wang, K. Wu, Z. Yu. *Organometallics*, **35**, 1251 (2016). (b) S.P. Shan, T.T. Dang, A.M. Seayad, B. Ramalingam. *ChemCatChem*, **6**, 808 (2014). (c) A.B. Enyong, B. Moasser. *J. Org. Chem.*, **79**, 7553 (2014).

[2] (a) C.S. Cho, B.T. Kim, H.S. Kim, T.J. Kim, S.C. Shim. *Organometallics*, **22**, 3608 (2003). (b) C. Xu, L.Y. Goh, S.A. Pullarkat. *Organometallics*, **30**, 6499 (2011).

[3] (a) T. Miura, O. Kose, F. Li, S. Kai, S. Saito. *Chem. Eur. J.*, **17**, 11146 (2011). (b) D. Gnanamgari, E.L.O. Sauer, N.D. Schley, C. Butler, C.D. Incarvito, R.H. Crabtree.

Organometallics, **28**, 321 (2009).

[4] X. Chang, L.W. Chuan, L. Yongxin, S.A. Pullarkat. *Tetrahedron Lett.*, **53**, 1450 (2012).

[5] C.S. Cho, W.X. Ren, S.C. Shim. *Bull. Korean Chem. Soc.*, **26**, 1611 (2005).

[6] K. Shimizu, R. Sato, A. Satsuma. *Angew. Chem. Int. Ed.*, **48**, 3982 (2009).

[7] X. Liu, S.R. Ding, L. He, M.Y. Liu, Y. Cao, Y.H. He, N.K. Fan. *ChemSusChem*, **6**, 604 (2013).

[8] (a) J. Yang, X. Liu, D.L. Meng, H.Y. Chen, Z.H. Zong, T.T. Feng, K. Sun. *Adv. Synth. Catal.*, **354**, 328 (2012). (b) B.T. Jahromi, A.N. Kharat. *J. Coord. Chem.*, **66**, 3498 (2013). (c) S. Arunachalam, N.P. Priya, C. Saravanakumar, C. Jayabalakrishnan, V. Chinnusamy. *J. Coord. Chem.*, **63**, 1795 (2010). (d) N. Thilagavathi, A. Manimaran, C. Jayabalakrishnan. *J. Coord. Chem.*, **63**, 1252 (2010).

[9] (a) X. Gong, H. Zhang, X. Li. *Tetrahedron Lett.*, **52**, 5596 (2011). (b) S.P. Shan, T.T. Dang, A.M. Seayad, B. Ramalingam. *ChemCatChem.*, **6**, 808 (2014). (c) X.F. Yin, H. Lin, A.Q. Jia, Q. Chen. Q.F. Zhang. *J. Coord. Chem.*, **66**, 3229 (2013).

[10] (a) M.G. Mura, S. Rajamaki, L.D. Luca, E. Cini, A. Porcheddu. *Adv. Synth. Catal.*, **357**, 576 (2015). (b) M. Rouffet, C.A.F. Oliveira, Y. Udi, A. Agrawal, I. Sagi, J.A. McCammon, S.M. Cohen. *J. Am. Chem. Soc.*, **132**, 8232 (2010). (c) J.L. Kim, I.S. Shin, H. Kim. *J. Am. Chem. Soc.*, **127**, 1614 (2005). (d) V. Bhalla, V. Vij, M. Kumar, P.R. Sharma, T. Kaur. *Org. Lett.*, **14**, 1012 (2012). (e) R.I. Khusnutdinov, A.R. Bayguzina, U.M. Dzhemilev. *J. Organomet. Chem.*, **75**, 768 (2014). (f) R. Klingenstein, P. Melnyk, S.R. Leliveld, A. Ryckebusch, C. Korth. *J. Med. Chem.*, **49**, 5300 (2006).

[11] (a) A. Arcadi, M. Chiarini, S.D. Giuseppe, F. Marinelli. *Synlett.*, 203 (2003). (b) G. Jones, Chemistry of Heterocyclic Compounds Quinolines, Part I, **32**, (Ed.: G. Jones), John Wiley & Sons, Hoboken (2008). (c) C.S. Cho, B.T. Kim, H.J. Choi, T.J. Kim, S.C. Shim. *Tetrahedron*, **59**, 7997 (2003).

[12] (a) T.C. Woon, L.K. Thompson, P. Robichaud. *Inorg. Chim. Acta*, **90**, 201 (1984). (b) W.J. Stratton. *Inorg. Chem.*, **9**, 517 (1970). (c) L. Cui, Y. Baek, S. Lee, N. Kwon, J. Yoon. *J. Mater. Chem.*, **4**, 2909 (2016). (d) X. Li, H. Sun, F. Yu, U. Florke, H.F. Klein. *Organometallics*, **25**, 4695 (2006). (e) Q.H. Wang, W. Weng, J.M. Liu. L.Z. Cai, G.C. Guo. *J. Coord. Chem.*, **59**, 485 (2006).

[13] (a) S.M. Wilkinson, T.M. Sheedy, E.J. New. *J. Chem. Educ.*, **93**, 351 (2016). (b) B.

Singh, U.R. Singh. *Cryst. Res. Technol.*, **26**, 1039 (1991). (c) M. Tirant, T.D. Smith, J.R. Pilbrow. *J. Coord. Chem.*, **16**, 263 (1987). (d) X. Gan, Z.F. Yao, J.F. Zhang, Z. Li. W.F. Fu. *J. Coord. Chem.*, **63**, 2800 (2010).

[14] (a) R. Ramachandran, G. Prakash, S. Selvamurugan, P. Viswanathamurthi, J.G. Malecki, V. Ramkumar. *Dalton Trans.*, **43**, 7889 (2014). (b) R. Manikandan, P. Anitha, G. Prakash, P. Vijayan, P. Viswanathamurthi. *Polyhedron*, **81**, 619 (2014).

[15] (a) M. Nirmala, R. Manikandan, G. Prakash, P. Viswanathamurthi. *Appl. Organomet. Chem.*, **28**, 18 (2014). (b) P. Anitha, P. Viswanathamurthi, D. Kesavan, R.J. Butcher. *J. Coord. Chem.*, **68**, 321 (2015).

[16] (a) N. Ahmed, J.J. Levison, S.D. Robinson, M.F. Uttley. *Inorg. Synth.*, **15**, 45 (1974). (b) R.A.S. Delgado, W.Y. Lee, S.R. Choi, Y. Cho, M.J. Jun. *Transition Met. Chem.*, **16**, 241 (1991).

[17] Z. Xu, L.K. Thompson, D.O. Miller, H.J. Clase, J.A.K. Howard, A.E. Goeta. *Inorg. Chem.*, **37**, 3620 (1998).

[18] G.M. Sheldrick. *Acta Crystallogr., Sect. A*, **64**, 112 (2008).

[19] S. Gowri, M. Muthukumar, S. Krishnaraj, P. Viswanathamurthi, R. Prabhakaran, K. Natarajan. *J. Coord. Chem.*, **63**, 524 (2010).

[20] G. Prakash, R. Manikandan, P. Viswanathamurthi, K. Velmurugan, R. Nandhakumar. *J. Photochem. Photobiol.*, **B 63**, 138 (2014).

[21] G. Prakash, R. Ramachandran, M. Nirmala, P. Viswanathamurthi, J. Sanmartin. *Inorg. Chim. Acta*, **427**, 203 (2015).

[22] (a) P. Satyanarayana, G.M. Reddy, H. Maheswaran, M.L. Kantam. *Adv. Synth. Catal.*, **355**, 1859 (2013). (b) R. Martınez, D.J. Ram, M. Yus. *Tetrahedron*, **62**, 8982 (2006).

[23] B.T. Kim, H.S. Kim, T.J. Kim, S.C. Shim. *Organometallics*, **22**, 3608 (2003).

[24] (a) D. Wang, X.Q. Guo, C.X. Wang, Y.N. Wang, R. Zhong, X.H. Zhu, L.H. Cai, Z.W. Gao, X.F. Hou. *Adv. Synth. Catal.*, **355**, 1117 (2013). (b) K.I. Fujita, C. Asai, T. Yamaguchi, F. Hanasaka, R. Yamaguchi. *Org. Lett.*, **7**, 4017 (2005).

[25] H.W. Cheung, T.Y. Lee, H.Y. Lui, C.H. Yeung, C.P. Lau. *Adv. Synth. Catal.*, **350**, 2975 (2008).

[26] (a) A. Prades, M. Viciano, M. Sanau, E. Peris. *Organometallics*, **27**, 4254 (2008). (b) R. Martınez, D.J. Ramon, M. Yus. *Tetrahedron*, **62**, 8982 (2006).

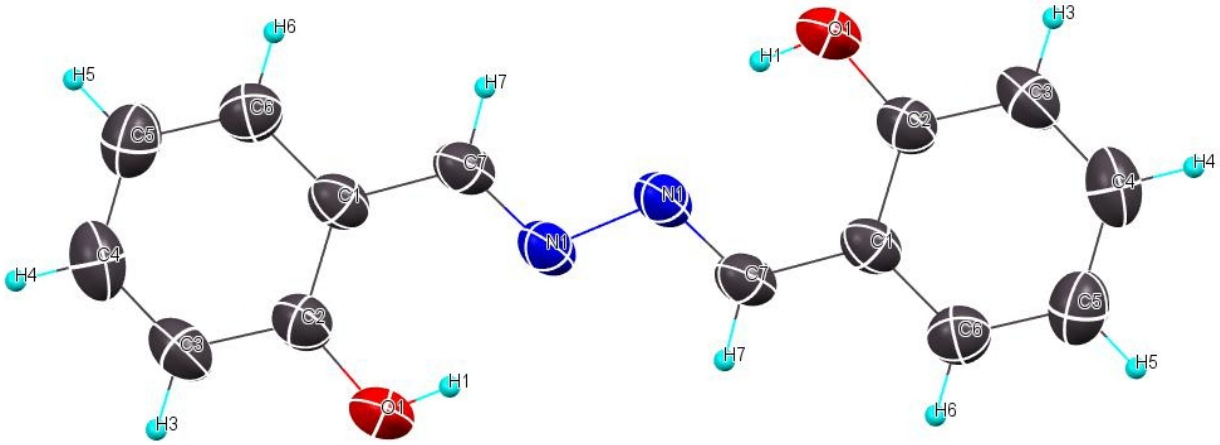

Figure 1. Perspective view (50% probability ellipsoids) of $\mathbf{H_2L_1}$ with atom numbering scheme.

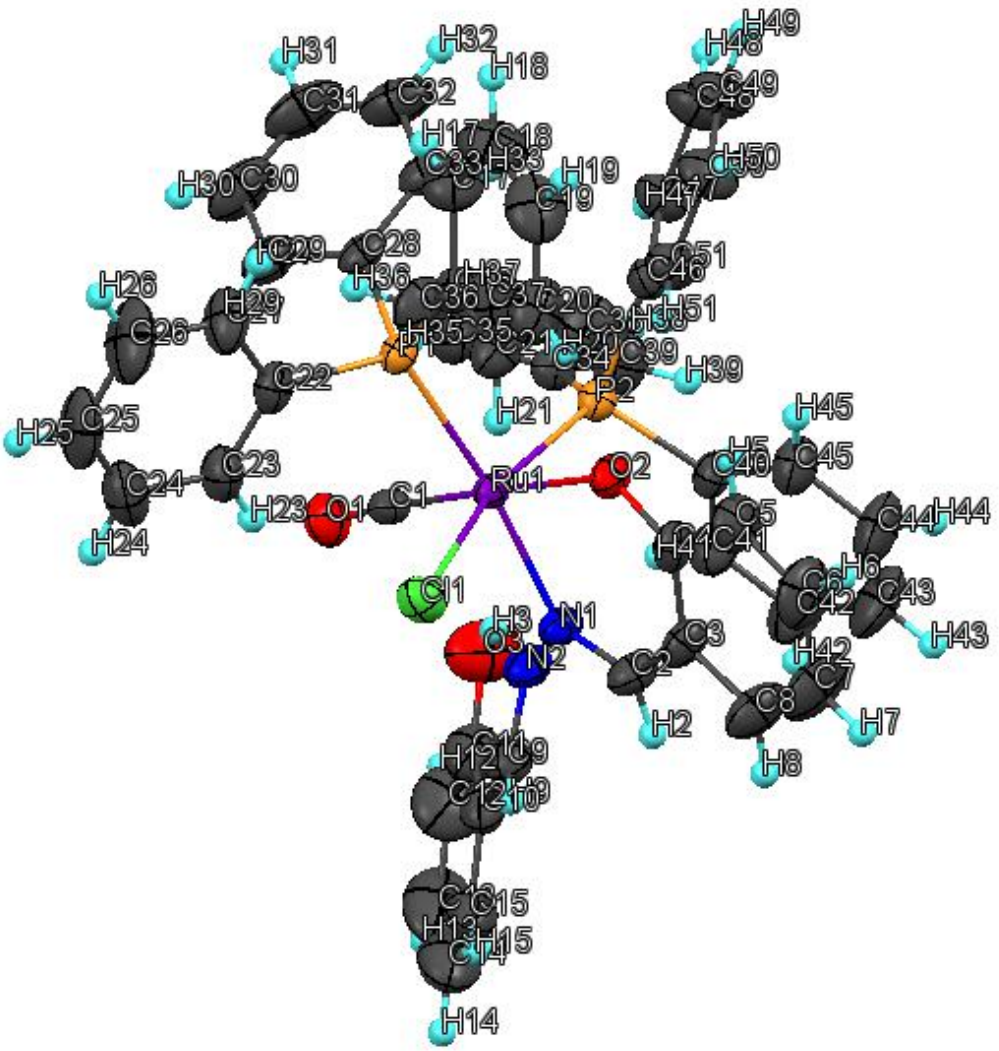

Figure 2. Perspective view (50% probability ellipsoids) of **1** with atom numbering scheme.

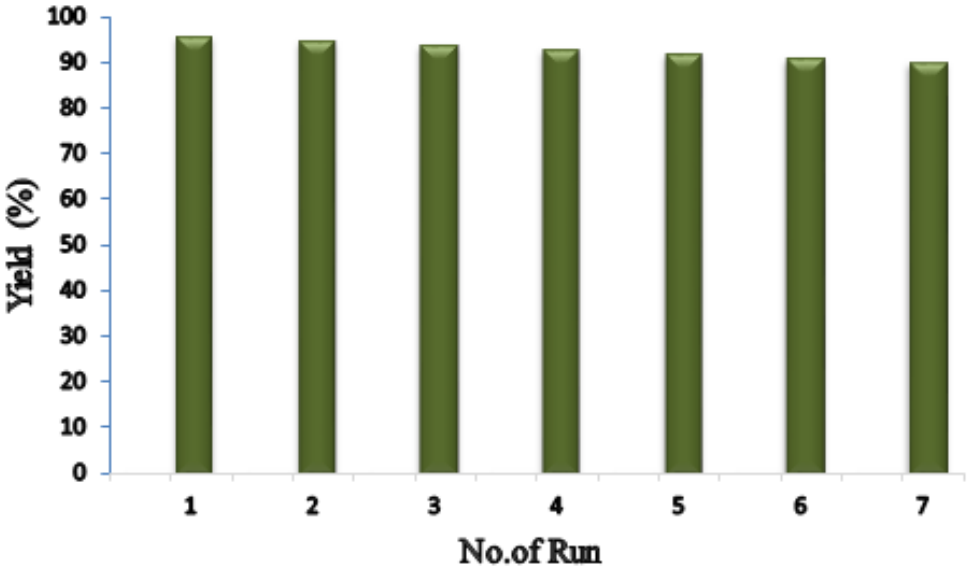

Figure 3. Recyclability of **1** using 1-phenyl ethanol and benzyl alcohol.

Table 1. Crystal data and structure refinement for $\mathbf{H_2L_1}$.

Compound	$\mathbf{H_2L_1}$	**1**
Empirical formula	$C_{14}H_{12}N_2O_2$	$C_{53}H_{43}N_3O_3ClP_2Ru$
Formula weight	240.26	969.37
T (K)	295	295 K
λ (Å)	0.71073	0.71073
Crystal system	Monoclinic	Monoclinic
Space group	*P21/n*	*P21/c*
Unit cell dimensions (Å, °)		
a (Å)	8.553(2)	18.4179(7)
b (Å)	6.3005(13)	10.5542(4)
c (Å)	11.825(3)	24.3652(8)
α (°)	90	90
β (°)	108.14(3)	101.896(4)
γ (°)	90	90
Volume ($Å^3$)	605.6(3)	4634.5(3)
Z	2	4
Calculated density (g cm^{-3})	1.318	1.389
Absorption coefficient (mm^{-1})	0.090	0.512
F(000)	252	1992.0
θ range for data collection (°)	3.521-29.422	3.372-29.488
Index ranges	-8<=h<=11	-25<=h<=25
	-5<=k<=8	-14<=k<=14
	-16<=l<=11	-33<=l<=33
Reflections collected	2739	28559
Independent reflections (R_{int})	1430 (0.0503)	11131 (0.0931)
Data / restraints / parameters	1430 / 0 / 84	11131 / 0 / 570
Goodness-of-fit on F^2	1.061	1.029
Final R indices [I > 2σ(I)]	R_1 = 0.0726	R_1 = 0.0444
	wR_2 = 0.1762	wR_2 = 0.0820
R indices (all data)	R_1 = 0.1318	R_1 = 0.0767
	wR_2 = 0.2536	wR_2 = 0.0931

Table 2. Selected bond lengths (A) and angles (°) for $\mathbf{H_2L_1}$ and **1** with the optimized geometrical values.

$\mathbf{H_2L_1}$	X-ray	**1**	X-ray
O(1)–C(2)	1.346(3)	C(1)–Ru(1)	1.839(3)
N(1)–N(1)	1.402(4)	N(1)–Ru(1)	2.110(2)
N(1)–C(7)	1.280(3)	O(2)–Ru(1)	2.0759(17)
C(1)–C(2)	1.399(4)	P(1)–Ru(1)	2.3808(7)
C(1)–C(6)	1.393(3)	P(2)–Ru(1)	2.3594(7)
C(1)–C(7)	1.446(4)	Cl(1)–Ru(1)	2.4459(7)
C(2)–C(3)	1.389(4)		
C(3)–C(4)	1.362(4)	P(1)–Ru1–Cl(1)	88.57(2)
C(4)–C(5)	1.390(4)	O(2)–Ru(1)–Cl(1)	83.20(5)
C(5)–C(6)	1.370(4)	O(2)–Ru(1)–P(1)	93.97(5)
		O(2)–Ru(1)–N(1)	86.78(7)
C(2)–C(1)–C(7)	121.6(2)	N(1)–Ru(1)–Cl(1)	82.88(6)
C(6)–C(1)–C(2)	118.5(2)	N(1)–Ru(1)–P(1)	171.28(6)
C(6)–C(1)–C(7)	120.0(2)	N(1)–Ru(1)–P(2)	89.25(6)
O(1)–C(2)–C(1)	122.3(2)	C(1)–Ru(1)–Cl(1)	97.26(8)
O(1)–C(2)–C(3)	118.4(2)	C(1)–Ru(1)–P(1)	88.14(8)
C(3)–C(2)–C(1)	119.3(3)	C(1)–Ru(1)–P(2)	94.32(8)
C(4)–C(3)–C(2)	121.0(3)	C(1)–Ru(1)–O(2)	177.86(9)
C(3)–C(4)–C(5)	120.5(3)	C(1)–Ru(1)–N(1)	91.19(10)
C(6)–C(5)–C(4)	118.8(3)	C(1)–Ru(1)–Cl(1)	97.26(8)
C(5)–C(6)–C(1)	121.9(3)	C(1)–Ru(1)–P(1)	88.14(8)
N(1)–C(7)–C(1)	121.3(2)	C(1)–Ru(1)–P(2)	94.32(8)

Table 3. Screening and optimization of solvents, bases and time for β-alkylation of secondary alcohols with primary alcohol catalyzed by **1**[a].

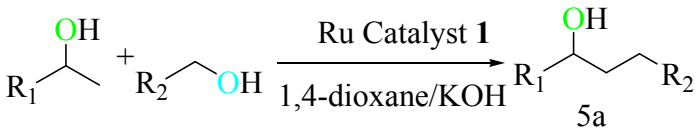

Entry	Solvent	Base (mol%)	Time (h)	Yield (%)[b]
1	---	KOH	18	19[c]
2	Toluene	KOH	21	87
3	Benzene	KOH	22	84
4	1,4-Dioxane	KOH	8	92
5	MeCN	KOH	15	27
6	DMF	KOH	12	71
7	DMSO	KOH	10	76
8	EtOH	KOH	17	59
9	H_2O	KOH	16	61
10	1,4-Dioxane	---	24	27[d]
11	1,4-Dioxane	Na_2CO_3	13	56
12	1,4-Dioxane	K_2CO_3	19	64
13	1,4-Dioxane	KO*t*Bu`	10	68
14	1,4-Dioxane	$NaNH_2$	12	72
15	1,4-Dioxane	NaOH	11	84
16	1,4-Dioxane	KOH	10	92
17	1,4-Dioxane	KOH	12	93
18	1,4-Dioxane	KOH	14	93
19	1,4-Dioxane	KOH	12	17[e]

[a] All reactions were carried out at 100 °C using R_1 = 1-phenylethanol (2.5 mmol), R_2 = benzyl alcohol (2.5 mmol), catalyst **1** (1 mol%), and base (2.5 mmol) in 1,4-dioxane (1 mL).

[b] Yields were calculated after isolation of the product through column chromatography using silica gel (200-400 mesh).

[c] The reaction was performed under solvent-free conditions.

[d] The reaction was performed under base-free conditions.

[e] The reaction was performed under without catalyst conditions.

Table 4. Effect of substitution and catalyst loading on *β*-alkylation of 1-phenyl ethanol with benzyl alcohol[a].

Entry	Catalyst	(mol%)	TON[b]	TOF[c]	Yield (%)[d]
1	1	0.25	256	32	64
2	1	0.5	158	20	79
3	1	1.0	92	12	92
4	1	1.5	60	8	90
5	2	1.0	90	11	89
6	3	1.0	84	11	84
7	4	1.0	77	10	77

[a] Reactions were carried out using 1-phenyl ethanol (2.5 mmol), benzyl alcohol (2.5 mmol), KOH (1 mol%), catalysts **1**-**4** at 100 °C for 8 h in 1,4-dioxane (1 mL).

[b] (TON) = (mmol of product)/(mmol of catalyst) after time *t*.

[c] TOF = TON/Time.

[d] Yields were calculated after isolation of the alcohol product through column chromatography using silica gel (200-400 mesh).

Table 5. *β*-Alkylation of different secondary alcohols with primary alcohols under optimized conditions[a].

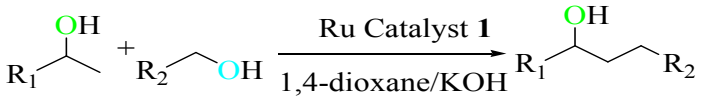

Entry	R_1	R_2	Product	Yield (%)[b]	TOF[c]
1	C_6H_5	C_6H_5	5a	92	12
2	C_6H_5	$CH_3(CH_2)_4$	5b	82	10
3	C_6H_5	$(CH_3)_2CHCH_2$	5c	71	9
4	C_6H_5	1-Naphthyl	5d	76	10
5	C_6H_5	4-$CH_3OC_6H_4$	5e	84	11
6	CH_3CH_2	C_6H_5	5f	89	11
7	CH_3CH_2	$CH_3(CH_2)_4$	5g	78	9
8	CH_3CH_2	$(CH_3)_2CHCH_2$	5h	68	9
9	CH_3CH_2	1-Naphthyl	5i	73	9
10	CH_3CH_2	4-$CH_3OC_6H_4$	5j	67	8
11	$CH_3C_6H_4$	C_6H_5	5k	84	11
12	$CH_3C_6H_4$	$CH_3(CH_2)_4$	5l	80	10
13	$CH_3C_6H_4$	$(CH_3)_2CHCH_2$	5m	73	9
14	$CH_3C_6H_4$	1-Naphthyl	5n	69	9
15	$CH_3C_6H_4$	4-$CH_3OC_6H_4$	5o	62	8

[a] All reactions were performed using 2.5 mmol of each alcohols, catalyst **1** (1 mol%), and base (2.5 mmol) in 1,4-dioxane (1 mL), at 100 °C.

[b] Yields were calculated after isolation of the alcohol product through column chromatography using silica gel (200-400 mesh).

[c] TOF = TON/Time, time fixed 8 h.

Table 6. Synthesis of quinolines from 2-aminobenzyl alcohol and secondary alcohol[a].

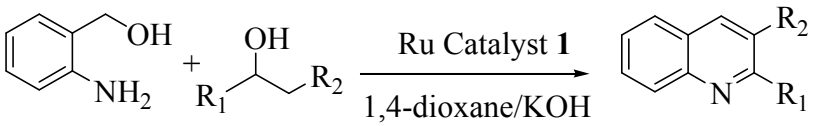

Entry	R_1	R_2	Product	Yield (%)[b]	TOF[c]
1	C_6H_5	H	6a	95	12
2	$CH_3C_6H_4$	H	6b	94	12
3	$CH_3OC_6H_4$	H	6c	82	10
4	CH_3CH_2	H	6d	90	11
5	Naphthyl	H	6e	89	11
6	2-Furanyl	H	6f	79	10
7	C_6H_5	CH_3	6g	89	11
8	C_6H_5	$C_6H_5CH_2CH_2$	6h	75	9
9	C_6H_5	$CH_3(CH_2)_5$	6i	64	8

[a] All reactions were performed using 2.5 mmol of each alcohol, catalyst **1** (1 mol%), and base (2.5 mmol) in 1,4-dioxane (1 mL) at 100 °C.

[b] Yields were calculated after isolation of the quinoline product through column chromatography using silica gel (200-400 mesh).

[c] TOF = TON/Time, time fixed 8 h.

Graphical abstract